

**UNIVERSIDAD DE LOS ANDES**

# **The expected shape of the Milky Way's dark matter halo**

by

**Jesus David Prada Gonzalez**

A thesis submitted in partial fulfillment for the  
degree of Master of Sciences in Physics

in the  
Faculty of Sciences  
Physics Department

April 2018

UNIVERSIDAD DE LOS ANDES

## *Abstract*

Faculty of Sciences  
Physics Department

Master of Sciences

by Jesus David Prada Gonzalez

The shape of the Dark Matter (DM) structure (halo) in which a galaxy is embedded is heavily determined by the anisotropic accretion of mass from its specific environment. Therefore, the shape of a galaxy's halo is an important feature to inquire about its formation history and the relation of DM and gas within it. In this work we study the shape of the DM halo of Milky Way-like galaxies from the Auriga simulations. We focus on the radial and time dependence. We found that, on DM-only and Magnetohydrodynamic (MHD) simulations, the shape of the DM halo is more triaxial in the inner-skirts than in the outer-skirts. We compared simulations with and without gas and verified that the presence of visible matter has an effect of rounding the DM halo which is amplified for smaller radii, where the gravitational potential of the galactic disk becomes more significant. Regarding the effect of time on the DM halo shape, we corroborated that it is well-conserved in comoving units until  $z \approx 2$ . This means that probing the halo shape at the virial radius in physical units for different redshifts is nearly equivalent to probing the shape at different radii at redshift 0. These results are in accordance with previous work on cosmological and galactic-size simulations, and may serve as guidelines to improve observational constraints on our MW DM halo.

UNIVERSIDAD DE LOS ANDES

## *Abstract*

Faculty of Sciences  
Physics Department

Master of Sciences

by Jesus David Prada Gonzalez

La forma de la estructura (halo) de Materia Oscura en la cual está embebida una galaxia es altamente determinada por la acreción anisotrópica de materia en el entorno específico en el que ésta se encuentra. Es por esto que la forma del halo de una galaxia es una característica importante para indagar sobre su historia de formación y la relación entre Materia Oscura y gas dentro de ella. En este trabajo estudiamos la forma de los halos de materia oscura en galaxias de tipo Vía Láctea del catálogo de simulaciones Auriga. Nos centramos principalmente en su dependencia radial y temporal. Hemos encontrado, en simulaciones de sólo Materia Oscura y en simulaciones de Magneto-hidrodinámica, que la forma del halo es más triaxial en las partes de adentro que en las afuera. Al comparar simulaciones con y sin gas, verificamos que la presencia de materia visible tiene un efecto de redondeado sobre el halo de Materia oscura, el cual es amplificado en radios pequeños, donde el efecto gravitacional del disco galáctico se torna significante. En cuanto al efecto del tiempo en la forma del halo de Materia Oscura, hemos corroborado que esta se conserva en unidades comóviles hasta  $z \approx 2$ . Esto se ve reflejado en la aproximada equivalencia entre el muestreo de la forma en el radio virial en unidades físicas a diferentes redshifts y el muestreo a diferentes radios en la actualidad. Estos resultados son respaldados por trabajos previos en simulaciones de escala galáctica y cosmológica, y pueden servir como lineamientos para mejorar las mediciones de la forma del halo de Materia Oscura de nuestra Vía Láctea.

## *Acknowledgements*

I am grateful with my mother and brother who encouraged me to work hard and cheered me up in difficult moments. I am also truly thankful with my advisor Jaime Forero for all the doors he has opened for me and for being my scientific father. I express my gratitude to my dad, without whom my Physics career would not have been possible....

# Contents

<b>Abstract</b>	<b>ii</b>
<b>Resumen</b>	<b>iii</b>
<b>Acknowledgements</b>	<b>iv</b>
<b>List of Figures</b>	<b>vi</b>
<b>List of Tables</b>	<b>vii</b>
<b>1 Introduction</b>	<b>1</b>
1.1 About Dark Matter . . . . .	1
1.2 Theoretical background for DM . . . . .	3
1.3 Constraining the Milky Way's DM Halo . . . . .	5
1.4 State of the art on MW simulations . . . . .	7
1.5 Synergy between Theory, Observations and Simulations . . . . .	10
1.6 Outline . . . . .	11
<b>2 Remarks about our study</b>	<b>12</b>
2.1 The Auriga simulations . . . . .	12
2.2 Determining the halo shape . . . . .	13
<b>3 Our results</b>	<b>17</b>
3.1 Convergence Analysis . . . . .	17
3.2 The radial dependence of axial ratios . . . . .	20
3.2.1 The effect of gas on the halo shape . . . . .	22
3.3 Historical shape . . . . .	24
<b>4 Conclusions</b>	<b>28</b>
<b>Bibliography</b>	<b>30</b>

# List of Figures

2.1	Set of 30 MW-like simulations from Auriga, taken from <a href="http://auriga.its.org/">http://auriga.its.org/</a>	15
3.1	Level 3 (green) & 4 (pink) radial profiles of axial ratios for halo 6 (DM) & 21 (MHD). Here, it is clear that there is good agreement on the calculated quantities for both levels of resolution.	18
3.2	Level 3 (green) & 4 (pink) radial profiles of axial ratios for halo 16 (DM) & 23 (MHD). Here, axial ratios show slow convergence.	19
3.3	The few-particle effect on the axial ratios convergence for halo 24 (DM & MHD). Here level4 curves (magenta) are compared to the $3\sigma$ range (clear blue) of the random-sampled curves from level3 (solid blue). We deduce from the fractional difference (green) that discrepancies at $r >> 1\text{Kpc}$ cannot be explained solely with the few-particle bias.	20
3.4	DM density for inner (left) and outer (right) parts of the halo 27. We present both versions: DM (up) & MHD (down). The horizontal and vertical axes are aligned to the major and medium semi-axes respectively. Here, it is evident that this halo is more spherical at bigger radii and more triaxial at the central parts.	21
3.5	Radial profile for axial ratios and the triaxiality parameter $T = \frac{1-b/a}{1-c/a}$ from halo 27 and halo 16. These halos have a clear radial tendency towards sphericity (for smaller radii until $\approx 3\text{Kpc}$ ), which can be confirmed with the triaxiality parameter.	22
3.6	Axial ratios as shown on $c/a$ Vs $b/a$ . Each dot represents a halo shape at some radius. Some observational constraints are plotted alongside our results. Here, dots are clustered, proving the general tendency of halos to get rounder on the outer parts.	23
3.7	General tendency on the triaxial plane $c/a$ Vs $b/a$ . Some observational constraints are plotted alongside our results	24
3.8	Radial profile (comoving) of axial ratios for halo 16 in terms of redshift (color). This halo maintains its shape until $z \approx 1$ obviating the systematic rounding effect in time from asymmetric potentials.	25
3.9	Radial profile (comoving) of axial ratios for halo 21 in terms of redshift (color). This halo is disrupted around $z \approx 0.5$ which results in a certain loss of its shape memory.	26
3.10	Historic shape (color dots) Vs actual radial shape (solid black line) on the Triaxiality plane. Each colored dot represents a calculated shape at R Mean 200, for each redshift. It is clear that halos with memory (halo 16), unlike disrupted halos (halo 21), have correlation between their historical and radial profiles.	27

# List of Tables

- 2.1 Specifications of each level 4 galaxy (halo). The DM and MHD versions of each parameters are presented together. The columns of this table indicate: (1) Halo name, (2,3) Number of (millions) of DM particles belonging to the halo, (4,5) Mass per particle in  $10^5 M_\odot$ , (6,7) Virial radius (R TopHat 200) of the halo in Kpc, (8,9) Virial mass of the halo in  $10^{14} M_\odot$ . 14
- 2.2 Specifications of each level 3 galaxy (halo). The DM and MHD versions of each parameters are presented together. The columns of this table indicate: (1) Halo name, (2,3) Number of (millions) of DM particles belonging to the halo, (4,5) Mass per particle in  $10^5 M_\odot$ , (6,7) Virial radius (R TopHat 200) of the halo in Kpc, (8,9) Virial mass of the halo in  $10^{14} M_\odot$ . 15

*Dedicated To my Mother and my little brother. . .*

# Chapter 1

## Introduction

### 1.1 About Dark Matter

In observational astronomy it is possible to find measurements which are not reconcilable with the current understanding of physical theories. Sometimes, these measurements are the result of instrumental error or incorrect theoretical assumptions. However, since the early beginnings of the 20th century, we have found inconsistencies of observations with the accepted paradigm of physics that challenge the veracity of the Newtonian gravity or even its improved Einsteinian version at astronomical and cosmological scales.

We observe that objects are moving in a certain way that cannot be explained exclusively by the effect of gravitational forces of visible matter. Specifically, observations show that there is an immense lack of matter to explain the gravitational pull reflected on observed dynamics. To solve this problem there are two important hypothesis to study.

One of these hypothesis tries to reconcile these observations with Newtonian/Einsteinian gravity assuming it is completely valid in the cosmological context. Consequently, there must exist some kind of matter that exerts this missing gravitational pull, which we cannot see for some reason. We talk about Dark Matter (DM).

Since early as the 1930's, the DM hypothesis has been considered. It is known that pioneer Fritz Zwicky proposed its presence within the Coma cluster of galaxies to explain the cluster attachment despite the galactic huge velocities that would have made them escape [1]. At first, this proposal was not given much attention as there were many

other sources of errors to blame and these observations were not widely replicated. Nevertheless, as years passed, more and more inconsistencies could be explained with the use of this DM hypothesis. It is the case of the famous rotation curves [2–4] where the amount of visible matter on galaxies could not account for the centripetal acceleration associated with the tangential velocities of stars within a it. Later on, with a better understanding of the space-curving effect of matter predicted by general relativity it was possible to measure weak lensing (gravitational distortion of observed objects) through massive clusters of galaxies [5–7]. Again, this effect was estimated to be much dimmer compared to observations.

Less direct evidence of DM is related to structure formation and the observed Cosmic Microwave Background Radiation (CMBR) [8]. On one hand, the early stages of the universe were dominated by radiation, which heavily affected visible matter by preventing it to grow clumps (form structures) from small density anisotropies. Specifically, due to radiation, the speed of sound is very close to that of the speed of light, meaning that density perturbations must be large to not be dispersed as sound waves. These anisotropies would be evidenced on the CMBR as temperature fluctuations. It was corroborated that these anisotropies are not present, through precise samplings of the CMBR like the Wilkinson Microwave Anisotropy Probe (WMAP) [9, 10] and the Planck Collaboration et al. [11, 12]. In the absence of any other kind of pulling force or kind of matter with smaller speed of sound (unaffected by radiation), we would not have the same distribution of collapsed structures (stars, galaxies, clusters) we observe today.

Subsequently, second important hypothesis studies the possibility that our comprehension of gravity or dynamics erroneous at cosmological scales. Then we talk about theories of modified gravity. One of the most successful alternatives of DM are Modified-Newtonian Dynamical (MOND) theories, which modify Newton's inertia law [13]. If we apply this hypothesis to the previous mismatches, under a precise tuning of parameters, we could obtain the wanted consistency [14]. Although these theories may succeed in many galactic-regime predictions [15–17], they are extremely well constrained for small-scale regimes by Newtonian/Einsteinian gravity. This restricts the freedom with which this models may be adjusted to observations and makes them highly refutable. Some of the biggest problems these theories face are DM remnants that are necessary to completely reconcile predictions and observations [18, 19]. Furthermore, for these theories, the excess of gravitational pull must be centered at the visible-matter distribution, which may not be the case for collisions of galaxies where it is observed that collisionless DM may decouple from baryonic mass [7].

For these reasons, DM is the most widely accepted hypothesis to account for observational discrepancies. Nonetheless, a complete physical picture of DM is still missing and it is one of the biggest puzzles to fully understand the composition of our Universe. Many appealing candidates may be found in the context of Particle Physics, which motivate the existence different kinds of weak-interacting particles through interesting symmetric theories [20, 21].

## 1.2 Theoretical background for DM

In the search for the candidate particle that makes up DM, there have been various proposals from particle physics. One of the most obvious candidates was the neutrino, a lepton of extremely small mass at rest. Although neutrinos fulfilled the basic properties of DM, there were many problems when reconciling with observations. These problems come from the analysis of CMB that constrains that at early stages of the universe neutrinos would be relativistic [21, 22], which would result in a non-hierarchical model of formation. Other problems include constraints on the density of neutrinos [9], which is not enough to account for missing matter. This kind of very-light DM candidates whose thermal energy significantly affects the proper growth of density anisotropies in the early universe, are known as Hot Dark Matter (HDM).

If we assume the existence of a heavier particle as a DM candidate, then these particles would not be relativistic at early stages and therefore they would support a hierarchical model of formation [8, 23]. In this case, we refer to this particles as Cold Dark Matter (CDM). Given its consistency with the observable universe, CDM is the most accepted candidate as the principal constituent of DM.

Given that CDM has negligible thermal energy, it is usually modeled as a set of gravitating collisionless particles, or, in the continuous case, as a collisionless self-gravitating Boltzmann fluid (1.1). As a consequence, neither the fluid/particle nor its interaction force possess a well-defined scale parameter. In other words, by a simple rescaling of position and time, we would arrive to an equivalent system. This characteristic of self-similarity is widely used on theoretical frameworks to simplify the calculations and imply that, many properties of DM structures are self-similar. For instance, on one hand Schechter used this argument to analyze the statistics of mass functions in a self-similar universe of DM [24] which has a very precise matching with observations. On the other hand, Bardeen used this self-similarity to analyze the evolution of random Gaussian

fluctuations of the DM density field [25], resulting in a theoretical framework that is a strong foundation for any work on the analysis of DM structures.

$$\frac{d\rho}{dt} = \frac{\partial\rho}{\partial t} + \vec{v} \cdot \frac{\partial\rho}{\partial\vec{x}} - \frac{\partial\Phi}{\partial\vec{x}} \cdot \frac{\partial\rho}{\partial\vec{v}}. \quad (1.1)$$

By means of example, using a computational approach, Navarro et al. discovered that DM halos (galactic sized clusters of DM) are ruled by a universal double-power law (1.2), which was independent of the size of the halo or the used cosmology [26–29]. This is expected from the self-similarity properties of DM, although it differs from the previously theoretically predicted single-power law [30, 31].

$$\frac{\rho(r)}{\rho_{crit}} = \frac{\delta_c}{(r/r_s)(1+r/r_s)^2}. \quad (1.2)$$

Now, collisionless models for CDM are a good approximation to model star dynamics or other cosmological objects with negligible cross-section, such as Black Holes (BH). Let us take, for example, the Boltzmann transport equation (1.1) in a convenient set of coordinates to analyze the dynamics of stars in axisymmetric galaxies. If we get rid of the phase-space density function  $f(\vec{x}, \vec{v})$  we can obtain an expression for stellar dynamics in terms of observable quantities such as the velocity means  $\bar{v}_r, \bar{v}_z, \bar{v}_\phi$ , the velocity correlation matrix  $\sigma$ , the spatial-density field  $\rho$  and the gravitational accelerations  $a_r, a_z, a_\phi$ . These equations are called Jeans equations in honor of James Jean who was the first to apply this knowledge in the cosmological context [32]. For the case of an axisymmetric stable system [33], these equations read:

$$\begin{aligned} a_r &= \sigma_{rr}^2 \frac{\partial \ln \nu}{\partial r} + \frac{\partial \sigma_{rr}^2}{\partial r} + \sigma_{rz}^2 \frac{\partial \ln \nu}{\partial z} + \frac{\partial \sigma_{rz}^2}{\partial z} + \frac{\sigma_{rr}^2}{r} - \frac{\sigma_{\phi\phi}^2}{r} - \frac{\bar{v}_\phi^2}{r} \\ a_z &= \sigma_{rz}^2 \frac{\partial \ln \nu}{\partial r} + \frac{\partial \sigma_{rz}^2}{\partial r} + \sigma_{zz}^2 \frac{\partial \ln \nu}{\partial z} + \frac{\partial \sigma_{zz}^2}{\partial z} + \frac{\sigma_{rz}^2}{r}, \end{aligned} \quad (1.3)$$

where the angular acceleration is null for stability reasons and the the spatial density  $\rho$  is encoded in the stellar number density distribution  $\nu$ .

In this case, the gravitational potential  $\Phi$  which produces the corresponding accelerations. These accelerations may be obtained by the integration of visible matter, but, as expected, they are underestimated. In this case we have a precise theoretical framework

to deduce the missing distribution of DM from stellar observable properties.

### 1.3 Constraining the Milky Way’s DM Halo

So far, DM presence can only be measured through its gravitational effect on the surrounding visible matter. One of best the astronomical systems that can be used to probe DM on astronomical scales is our own galaxy: the Milky Way (MW). Probing the DM density field around our galaxy (it’s so-called DM halo) can shed light on the nature of DM [34, 35] and our galaxy history of formation [36–38].

DM haloes have two important features that could be constrained. On one hand there is the universal density profile on equation (1.2) [29]. On the other hand, there is the halo shape, which is directly related to its spin. According to the hierarchical model of structure formation, due to the anisotropic history of accretion DM haloes are triaxial and therefore, their shape and spin are important characteristics to **diagnose** their formation history [25, 39].

In this sense, it is of special interest to constrain the DM halo shape of the only cosmological object of which we have a three-dimensional view from inside: our Milky Way. However, this is a very difficult labour given the observational restrictions. Many approaches have been made to constrain the MW’s DM shape. One of them is to make use of theoretical models that relate the content of matter of our galaxy with the gravitational potential.

For example, Loebman et al. [33] used the axisymmetric Jean’s equations on (1.3). The observed accelerations cannot be completely explained by visible matter only and DM presence is needed. Loebman et al. estimated that, around 20Kpc, the DM halo must be perfectly oblate with axis ratio of  $q_{DM} = 0.47 \pm 0.14$  to account for this discrepancy.

Nevertheless, this axial symmetry is inherited from the use of axisymmetric Jean’s equations. Although this is a strong assumption, a more general method is much more difficult to implement given the difficulty to obtain the needed data from observations. Even authors acknowledge that:

... while it is premature to declare  $q_{DM} = 0.47 \pm 0.14$  as a robust measurement of the dark matter halo shape, it is encouraging that the simulation is at least qualitatively consistent with SDSS data in so many aspects.

This shows that this field of study is still young and any constraint may lead us to a better understanding of our MW's DM halo shape.

A more stronger approach is to use the streams of close dwarf galaxies that have been deformed by the gravitational potential of the MW. This effect is very important because the torque generated by the anisotropy in our halo is sensible to its shape parameters [40–42]. In fact, it is known that a static axisymmetric halo cannot simultaneously explain all the features of the Sagittarius leading arm [40].

In this context Law and Majewski 2010 proposed an analytical model of the MW consisting of a fixed analytical gravitational potential formed by a Miyamoto-Nagai [43] disk, a Hernquist spheroid and a logarithmic halo. This halo is triaxial and is characterized by its axial ratios and orientation. Given all these parameters, the Sagittarius stream was simulated and evolved forward and backwards in time for various choices of the halo parameters. The best fit, compared to a detailed study of the observational properties of the Sagittarius stream, was found at a minor/major axis ratio  $(c/a)_\Phi = 0.72$  and intermediate/major axis ratio  $(b/a)_\Phi = 0.99$ . The minor axis of this triaxial halo was found to be pointing in some direction contained in the galactic disk plane.

This sophisticated model succeeded at simultaneously reproducing the radial velocity and angular position trends of the Sagittarius leading arm, which were troublesome to model with simpler approaches. Nevertheless, the coexistence of a triaxial DM halo and an axisymmetric galactic disk is not supported by Cold Dark Matter (CDM) models [44]. Specifically, it is expected that the DM and gas distributions are correlated in the sense that matter is accreted from the same cosmic structures as is DM. Therefore, gas and DM must have aligned angular momenta to certain extent, i.e. for minor axes must be aligned. Furthermore, to guarantee stability reasons and a historical interaction, DM distributions should be axisymmetric in the presence of an axisymmetric disk potential [45].

Law and Majewski comment in their paper:

... by no means do they (results) represent best-fit models in a statistical sense. Therefore, the predictions made cannot be considered exclusive or definitive but serve to guide where future observations could focus to distinguish between various models.

Particularly, this discrepancy with the current CDM paradigm may be a feature of the specific model. Other important observational constraints were dismissed in this study, such as the non-symmetric influence of the Large Magellanic Cloud (LMC). This feature may obviate the triaxial halo and produce a more CDM-consistent model. However, observationally obtaining the detailed information of the LMC needed for this kind of research is extremely difficult.

Studies of this kind are by nature non-exact due to the difficulty in obtaining precise information from observations. In observations, we take 2-dimensional snapshots of the sky and loose resolution of the radial density field due to screening of matter. This makes the process of obtaining a three-dimensional view of a cosmological-scale object an extremely difficult endeavour. Furthermore, we can determine radial velocities with Doppler effect, but there is no obvious way of obtaining tangential velocities. Bearing this in mind, any study which is sensible to detailed observational parameters for obtaining non-direct measurements of the DM density field, will be either non-conclusive for reasonable-difficulty models, or must be extremely sophisticated to achieve a significantly exact result.

## 1.4 State of the art on MW simulations

To address the observational difficulties, there is an important field consisting in the modeling of the non-linear behaviour of matter. This is with the objective of numerically simulating the universe at a wide range of scales and produce systems of which we have full control of their parameters. In this sense, a computer may become a virtual cosmological laboratory, where we may run different experiments having control over their initial conditions, and in this way support or verify theoretical frameworks.

Cosmological simulations are usually restricted to modeling DM as a non-collisional fluids (1.1) and gas as an Eulerian collisional fluid (1.7). Efficiently solving these systems of non-linear equations, is an intricate puzzle and it is still an open and improving field of research. Difficulties in the modeling of these fluids arise from numerical instabilities

and the wide range of values that quantities take in the cosmological context, which may quickly expand in several orders of magnitude, becoming problematic numerical discontinuities. Depending on the current computing power, these simulations are limited to some resolution, which is adjustable to the specific objective of the research.

$$\frac{d\rho}{dt} + \rho \vec{\nabla} \cdot \vec{v} = 0 \quad (1.4)$$

$$\frac{d\vec{v}}{dt} = -\frac{\vec{\nabla}P}{\rho} - \vec{\nabla}\Phi \quad (1.5)$$

$$\frac{du}{dt} = -\frac{P}{\rho} \vec{\nabla} \cdot \vec{v} - \frac{\Lambda(\vec{u}, \rho)}{\rho} \quad (1.6)$$

$$P = (\gamma - 1)\rho u \quad (1.7)$$

In a historical context, numerical astrophysics have experienced a parallel growth with computing power and numerical methods. As we stated earlier, collisionless fluids are not restricted to the modeling of DM but can also be applied to cosmological objects with negligible cross-section. In this sense, as early as 1960's, it became possible for theoretical astrophysicists to run small-sized simulations of two-dimensional galaxies. This is the case of Miller and Pendergast [46] and Hohl and Hockney [47], who tried to recover the spiral stable form of galaxies like our MW. At this point, the computational power was not sufficient to even attempt a proper solution of collisional fluids. Even today, this requires extreme care and computational power. Consequently, to simulate dissipation effects of collision of gas clouds they emulated temperatures as random peculiar velocities of particles and implemented some cooling process in which some particles lose energy [48]. With this work, and some insight from Jerry Ostriker and James Peebles [45] it was demonstrated that galactic disks cannot be stable on their own and need some sort of additional radial pull (DM). In these simulations it was also verified that spiral branches of galaxies are a consequence of the propagation of small density fluctuations driven by dissipation of energy by gas clouds. Parallel to this work, it was also demonstrated by Toomre and Toomre [49] that these disruptions could also be caused by tidal forces of close encounters between galaxies.

Even with the advances of computational power following Moore's law, the numerical methods used to solve simulations quickly became obsolete year by year and needed to be pushed forward to an optimization of the computational resources. In this way, computational astrophysics evolved from brute-force  $N$ -body simulations to the use of tree-based simulations [50], to even dynamical-mesh simulations [51]. This co-evolution

between numerical methods and astrophysics together with the exponential growth of computational power, eventually made possible the performance of Cosmological-sized DM-only simulations such as Millennium which could reproduce the observed cosmological structures at a wide range of scales.

In this context, the analysis of gas was usually imprinted through the use of semi-analytic methods. They took the numerical output and performed analytical calculations to match the distribution of a certain number of visible-matter properties that we observe today [52, 53]. Although these semi-analytical methods did not trace the evolution of gas alongside with DM, it was the most realistic gas model that could be performed. By this time, numerical methods trying to actually simulate gas suffered from a process of over-cooling in which gas collapsed too quickly and did not produce stable galaxy-sized disk like we observe today [54].

This over-cooling process was understood to be a consequence of not having into account events of energy redistribution that stopped the rapid collapse. The principal sources of this energy transport are now known to be supernovae (SN) explosions, radiation from cosmic rays and the Active Galactic Nucleus (AGN). These terms are usually referred to as stellar feedback, radiation pressure and AGN feedback, respectively. They enclose modern physics processes which cannot be fully simulated and must be estimated with general recipes with some free parameters. For instance, in case of SNe explosions this process of energetic feedback is simulated by isotropically liberating some amount (free parameter) of kinetic energy (radial velocity recoil) as well as some amount of thermal energy (Temperature), to the surrounding gas cells.

A decade ago, these feedback processes were not as well understood as they are today. For this reason, it has been possible only until recently the simulation of an unprecedented set of 30 galactic-sized objects like our MW, tracing the evolution of normal matter alongside with DM with exceptional accuracy. This project is called Auriga, [55] and not only it has state-of-the-art energetic feedback physics, it is run with the novel hydrodynamic code AREPO [56]. This code combines a moving Voronoi tessellation with the finite volume approach and in this way, it solves the principal sources of numerical errors from both important paradigms of computational hydrodynamics in the cosmological context. Moreover, it is the first time that a consistent Magentic Field could be simulated in these kind of simulations [57].

## 1.5 Synergy between Theory, Observations and Simulations

In the CDM paradigm, we have fully theoretical studies [24, 25] principally focused in the analysis of Gaussian random fields and the properties of self-similarity that DM must possess. These theoretical frames are then supported by CDM simulations and, if possible, by observations. In fact, these theories are usually thoroughly verified and complemented through simulations, given their convenient malleability, before being directly applied to observations.

One good example of this synergy is evidenced in the work of Vera-Ciro et al. (2011-2013). In 2011, Vera-Ciro et al. studied the shape of a set of four MW-like DM-only galaxies from Aquarius simulations [58], with the objective of complementing the predictions of the CDM paradigm. Specifically, the hierarchical model of structure formation predicted that the halo shape must be correlated with the environment [59, 60]. However, theoretical studies of halo shapes are restricted to the correlations at redshift 0 and do not say much about their history of formation. Intuitively, it is expected that halo shapes vary with the radius taking into account that accretion occurs at progressively bigger radii in history and that the cosmic structures that determine environments evolve during that time. Due to the collisionless nature of DM, inner shells of the halo can interact with outer shells only in a gravitational way. This means that the historical shape must be conserved in the radial shape profile.

Vera-Ciro et al. showed in 2011 that the radial profile of the halo shape is indeed correlated with its accretion history and environment. Furthermore, due to the increase in the cross section of the halos, which contributes to the scattering of particles, at later stages and bigger radii, they become more oblate/spherical. These results helped to obtain more insight about the galactic dynamics of formation and also suggested some guidelines to improve Law and Majewski 2010 study.

In 2013, Vera-Ciro and Helmi proposed an improved study based on the one performed by Law and Majewski in 2010. They modeled a halo as perfectly oblate at inner regions, which transitions smoothly to a triaxial halo in the outer-skirts. With this, the angular momentum inconsistency of this constraint with the CDM model is solved. They found that this halo is triaxial in the outer skirts with a medium-to-major axis ratio of 0.9 and minor-to-major axis of 0.8, which is still very oblate regarding the CDM predictions.

However, besides solving some inconsistencies with the expected predictions, it demonstrated that small perturbations are important. Specifically, even when the Sagittarius stream samples the gravitational potential at the outer parts of the halo, where the shape of the inner regions should not be important, the outer shape is affected to compensate for the change in the regions from inside. This effect takes our attention to a relegated topic: the LMC. In fact, Vera-Ciro et al. demonstrated that the change in shape from the inner regions produces a torque comparable to that of the LMC, which should be taken into account in further researches.

This study comes from DM-only simulations and succeeded at improving previous constraints on the shape of our MW halo from a better understanding of DM. Taking into account the new and improved Auriga simulations, which can model gas alongside DM, our principal motivation in this work is to use these simulations validate previous knowledge about DM, as well as obtaining new insights on the DM-gas relation. Specifically, we want to verify how the shape of a DM halo is affected by radius, redshift and presence of gas.

## 1.6 Outline

This thesis is organized as follows: in Chapter 2 we present details about the Auriga simulations in which we perform our calculations, as well as the specifics of the shape-calculating method that we use for our purposes. In Chapter 3 we present our results. And Finally, in Chapter 3 we resume and discuss our work and its future projection.

# Chapter 2

## Remarks about our study

In this chapter we introduce some details of the Auriga simulations. Thereafter we give specific details about the method we use to characterize DM halos triaxiality.

### 2.1 The Auriga simulations

In this monograph we use the results of the state-of-the art Auriga simulations [55]. It selected a set of 30 isolated halos from the Evolution and Assembly of GaLaxies and their Environments (EAGLE) project [61]. Each halo was identified with the algorithm "Friend of Friends" (FOF) [62], that recursively links particles if they are closer than some distance threshold referred as linking length. EAGLE follows the evolution of fixed-mass particles of  $m_{\text{DM}} = 1.15 \cdot 10^7 M_{\odot}$  from  $z = 127$  to  $z = 0$ , adopting the  $\Lambda$ CDM model from the [11, Planck Collaboration et al. (2014)]. Here, the cosmological model  $\Lambda$ CDM consists of the coupling of the CDM paradigm with the cosmological constant  $\Lambda$  that portrays Dark Energy (DE) in an attempt to explain the accelerated expansion of the universe. This model is characterized by the Hubble constant  $H$  and the densities of the principal constituents of our universe, namely DE ( $\Omega_{\Lambda}$ ), DM ( $\Omega_m$ ) and baryons ( $\Omega_b$ ). The [11, Planck Collaboration et al. (2014)] used a precise sampling of the CMBR to constrain these cosmological parameters, resulting in the following values:  $\Omega_{\Lambda} = 0.693$ ,  $\Omega_m = 0.307$ ,  $\Omega_b = 0.048$  &  $H_0 = 67.77 \text{km s}^{-1} \text{Mpc}^{-1}$ .

These halos were randomly selected from a sample of the most isolated quartile of halos whose virial mass  $M_{200}$  varied between  $10^{12} M_{\odot}$  and  $2 \cdot 10^{12} M_{\odot}$ . This mass is defined as the mass enclosed within the virial radius  $R_{200}$  at which the density becomes 200 times the critical density of the universe. These halos were re-simulated by increasing

the mass resolution of the particles belonging to them and diminishing the resolution of the rest of the particles. This would efficiently simulate external gravitational effects over the studied structure while focusing on a high-resolution version of it.

Various versions of the same halo were simulated for different degrees of realism. All 30 halos were simulated within a level 4 degree of resolution defined for Aquarius simulations corresponding to  $\tilde{3} \cdot 10^6$  high resolution particles of  $\tilde{2.5} \cdot 10^5 M_\odot$ . The principal details of each of these halos are consigned on the table 2.1. From these halos, 6 of them where re-simulated at level 3 (higher) resolution taking into account a spatial factor of 2 in each dimension. For more information about level 3 halos, their details are printed on table 2.2. Furthermore, fore each halo in each level of resolution there are two versions of the simulation. One of them evolves only DM particles and the remaining one has into account magneto-hydrodynamical (MHD) physics, including DM. Taking this into account, we can compare the results from different levels of realism to obtain consistency in our analysis.

## 2.2 Determining the halo shape

The discretization of the DM density field into particles makes it difficult to perform some calculations that would require a more continuous distribution. Therefore, there is no trivial way to calculate the DM halo shape at a determined radius. There are different approaches to this problem, such as the use of an inertia tensor or the approximation to the respective contour surface. However, results from different methods do not differ much from each other [38]. In this work we follow the guidelines by [38, Vera-Ciro et al. 2011] which includes the use of the shape method proposed by [63, Allgood et al. 2006].

Allgood's method starts with particles enclosed within a sphere of initial radius  $r$ . We calculate the reduced inertia tensor:

$$I_{ij} = \sum_k \frac{x_k^{(i)} x_k^{(j)}}{d_k^2}, \quad (2.1)$$

whose components are weighted by the distance  $d^2 = x^2 + y^2 + z^2$ , so that each particle contribute with same importance to the sum regardless of their radius from the center.

Halo	$N_P/10^6$		$M_P/10^5 M_\odot$		$R_{vir}/\text{Kpc}$		$M_{vir}/10^{14} M_\odot$	
	DM	MHD	DM	MHD	DM	MHD	DM	MHD
halo 1	4.068	2.447	2.397	2.022	196.927	187.674	9.062	7.844
halo 2	5.625	5.457	2.481	2.093	235.094	233.934	15.418	15.191
halo 3	3.826	3.852	2.645	2.231	210.693	210.955	11.099	11.141
halo 4	4.585	4.530	2.590	2.185	219.378	215.438	12.529	11.866
halo 5	3.262	3.290	2.533	2.137	196.984	197.246	9.071	9.106
halo 6	3.184	3.110	2.337	1.972	191.840	189.342	8.378	8.054
halo 7	3.878	3.729	2.296	1.937	197.864	196.509	9.193	9.005
halo 8	2.772	2.796	2.451	2.068	190.716	191.764	8.231	8.368
halo 9	3.038	3.010	2.738	2.310	195.826	190.640	8.911	8.222
halo 10	2.700	2.751	2.541	2.144	187.139	188.147	7.777	7.904
halo 11	4.146	4.116	2.541	2.144	221.821	219.568	12.952	12.560
halo 12	2.865	2.908	2.645	2.231	192.280	192.038	8.436	8.404
halo 13	3.520	3.600	2.393	2.019	202.139	203.815	9.801	10.048
halo 14	4.200	4.475	2.499	2.108	215.535	218.927	11.882	12.453
halo 15	2.888	2.845	2.541	2.144	199.848	200.658	9.471	9.588
halo 16	3.821	3.871	2.499	2.108	212.590	212.632	11.401	11.408
halo 17	2.752	2.781	2.552	2.153	188.067	187.404	7.893	7.811
halo 18	3.770	3.624	2.738	2.310	201.124	207.293	9.655	10.571
halo 19	2.989	3.086	2.645	2.231	200.244	200.325	9.527	9.540
halo 20	3.903	3.822	2.481	2.093	210.097	211.423	11.005	11.214
halo 21	4.105	4.075	2.640	2.227	219.527	219.823	12.555	12.604
halo 22	2.794	2.766	2.625	2.215	188.363	184.801	7.931	7.489
halo 23	3.977	4.073	2.795	2.358	217.768	215.959	12.254	11.952
halo 24	4.466	4.426	2.522	2.127	217.440	215.147	12.199	11.817
halo 25	2.902	2.806	2.645	2.231	199.922	198.299	9.482	9.254
halo 26	4.610	4.716	2.506	2.115	219.984	218.939	12.633	12.454
halo 27	5.060	5.018	2.590	2.185	228.036	226.225	14.071	13.740
halo 28	4.184	4.276	2.645	2.231	216.979	217.997	12.121	12.294
halo 29	4.827	4.613	2.499	2.108	225.791	219.935	13.660	12.625
halo 30	3.268	3.112	2.579	2.176	195.043	194.741	8.805	8.763

TABLE 2.1: Specifications of each level 4 galaxy (halo). The DM and MHD versions of each parameters are presented together. The columns of this table indicate: (1) Halo name, (2,3) Number of (millions) of DM particles belonging to the halo, (4,5) Mass per particle in  $10^5 M_\odot$ , (6,7) Virial radius (R TopHat 200) of the halo in Kpc, (8,9) Virial mass of the halo in  $10^{14} M_\odot$ .

The diagonalization of this tensor yields the principal axes of the structure, as well as the eigen-quantities  $a > b > c$  which are proportional to the principal axes. However, if we characterize an ellipsoid taking into account only particles enclosed within a sphere, we are effectively miscalculating its triaxiality [63]. For this reason, we iteratively recalculate the inertia tensor taking into account the previously characterized ellipsoid.

AllGood et al. propose to use the eigenvalues  $a > b > c$  and their respective eigen-axes  $v_a, v_b, v_c$  to recalculate the inertia tensor over the particles enclosed by the ellipsoid with

Halo	$N_P/10^6$		$M_P/10^5 M_\odot$		$R_{vir}/\text{Kpc}$		$M_{vir}/10^{14} M_\odot$	
	DM	MHD	DM	MHD	DM	MHD	DM	MHD
halo 6	24.902	24.185	0.292	0.246	191.741	188.367	8.365	7.932
halo 16	29.750	30.334	0.312	0.263	212.622	212.542	11.406	11.395
halo 21	31.993	31.503	0.330	0.278	219.731	220.250	12.588	12.679
halo 23	31.379	31.618	0.349	0.295	217.793	213.358	12.259	11.524
halo 24	34.987	35.153	0.315	0.266	217.313	213.963	12.179	11.624
halo 27	39.617	39.056	0.324	0.273	227.908	223.484	14.048	13.244

TABLE 2.2: Specifications of each level 3 galaxy (halo). The DM and MHD versions of each parameters are presented together. The columns of this table indicate: (1) Halo name, (2,3) Number of (millions) of DM particles belonging to the halo, (4,5) Mass per particle in  $10^5 M_\odot$ , (6,7) Virial radius ( $R_{\text{TopHat 200}}$ ) of the halo in Kpc, (8,9) Virial mass of the halo in  $10^{14} M_\odot$ .

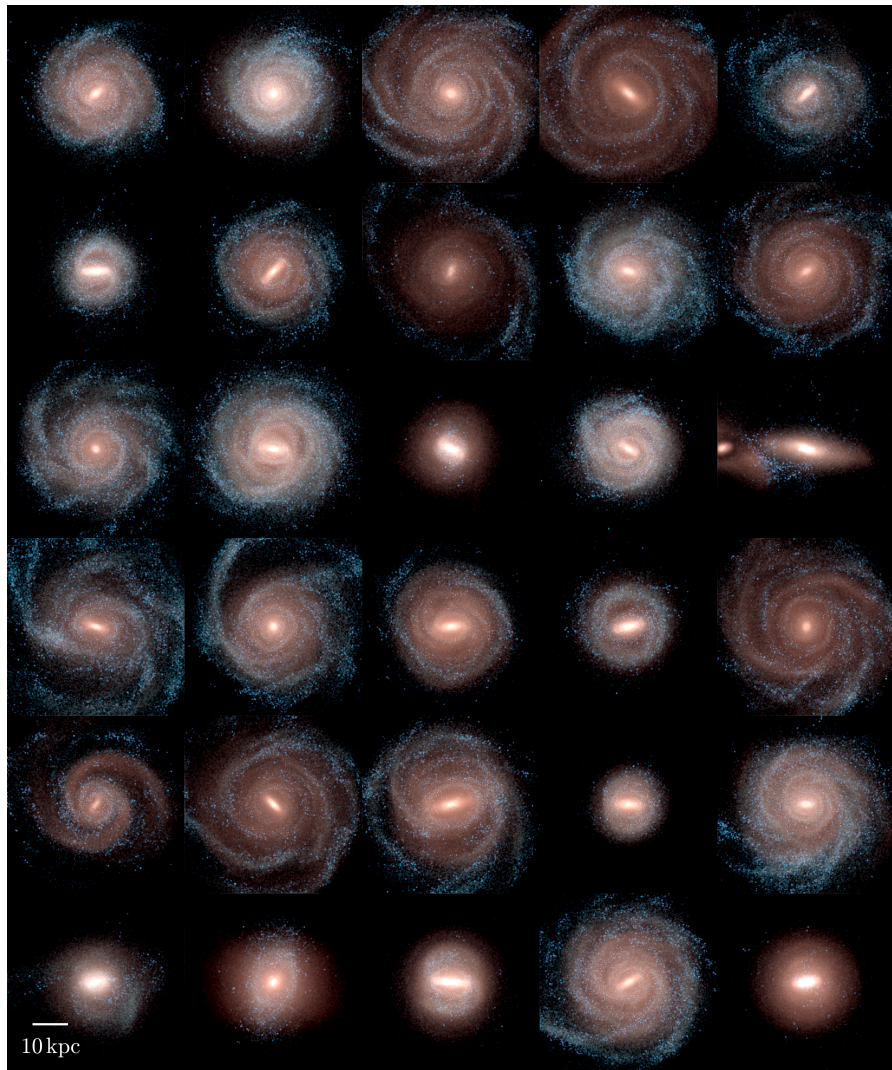


FIGURE 2.1: Set of 30 MW-like simulations from Auriga, taken from <http://auriga.h-its.org/>

principal axes (along the respective eigenvectors) equal to  $r, r/q, r/s$ , where ere  $q = b/a$  and  $s = c/a$  are the axial ratios. In other words, we repeat the process of calculating

the inertia matrix by taking into account particles within an ellipsoid with axial ratios given by the previous diagonalization. In this case, as the constant of proportionality is a free parameter, we choose to hold the size (not the direction) of the principal axis constant.

This method looks reliable and it would eventually converge to a more accurate characterization of the halo ellipsoid. However, we are computing the reduced inertia tensor by weighting the contributions with the spherical-metric distance  $d^2 = x^2 + y^2 + z^2$ , where particles within the same spherical surface are given the same importance. This means we are again introducing some error in the triaxiality of the structure. For this reason, on each iteration we must calculate the inertia tensor taking into account an elliptic metric:  $\bar{d}^2 = x^2 + y^2/q^2 + z^2/s^2$ , assuming  $x, y, z$  are the corresponding principal axes.

In case this concept of an elliptic metric is difficult to grasp, let us consider that, instead of converting the initial enclosing sphere to the halo ellipse, we are converting the halo ellipsoid into a sphere by performing scale transforms along the respective eigen-axes. From this point of view, we start our first-guess calculation of the ellipsoid by computing the reduced inertia tensor (2.1) for particles enclosed within a sphere of radius  $r$ . Then with the results of this first guess, we perform the following scale transform:

$$(x, y, z) \rightarrow (x', y', z') = (x, y/q, z/s) \quad (2.2)$$

$$q = b/a$$

$$s = c/a,$$

where we assumed the unit vectors  $\hat{x}, \hat{y}, \hat{z}$  are oriented at the principal elliptic axes. We then repeat the process of calculating the reduced inertia tensor and performing the scale transformation until we achieve a certain convergence criterion. We stop this iterative process when the sum of the fractional change in axes is less than  $10^{-6}$ . Finally, we obtain the shape of the halo at the geometric mean radius  $(abc)^{1/3}$ , which is not much different from the initial radius.

Notice that, for diagonalization purposes, calculating the inertia tensor with the scaled coordinates  $x', y', z'$  is equivalent to calculating it with the un-scaled coordinates  $x, y, z$ , using the elliptic-metric distance  $\bar{d}^2 = x^2 + y^2/q^2 + z^2/s^2$ .

# Chapter 3

## Our results

In this chapter we present the principal results of our work as well as some CDM-consistent phenomenology. First, we address convergence issues. Secondly, we study the relation of the axial ratios in terms of the radius. On third place, we show our results on the effect of baryons on the molding of the shape. Finally, we study the evolution of the radial profile of the axial ratios.

### 3.1 Convergence Analysis

One of the principal factors that may bias our study is the resolution of the simulations. Fortunately, Auriga simulations have level 3 and level 4 versions of 6 of the galaxies which we can use to analyze the numerical convergence of the results. Resolution may also affect our procedure for calculating halo shapes through the reduction of particles taken into account to calculate the inertia tensor.

To illustrate this, in figures 3.1 we compare the halo shape at redshift 0 for level 3 and level 4 simulations. In this case, we can say that there is good convergence of the studied quantities with very small numerical bias. However, this is not the case for every simulated halo.

By way of example, in figures 3.2 we present a halo where resolution significantly affected the shape. In this case, although the difference is not extreme, it requires attention and a more careful analysis.

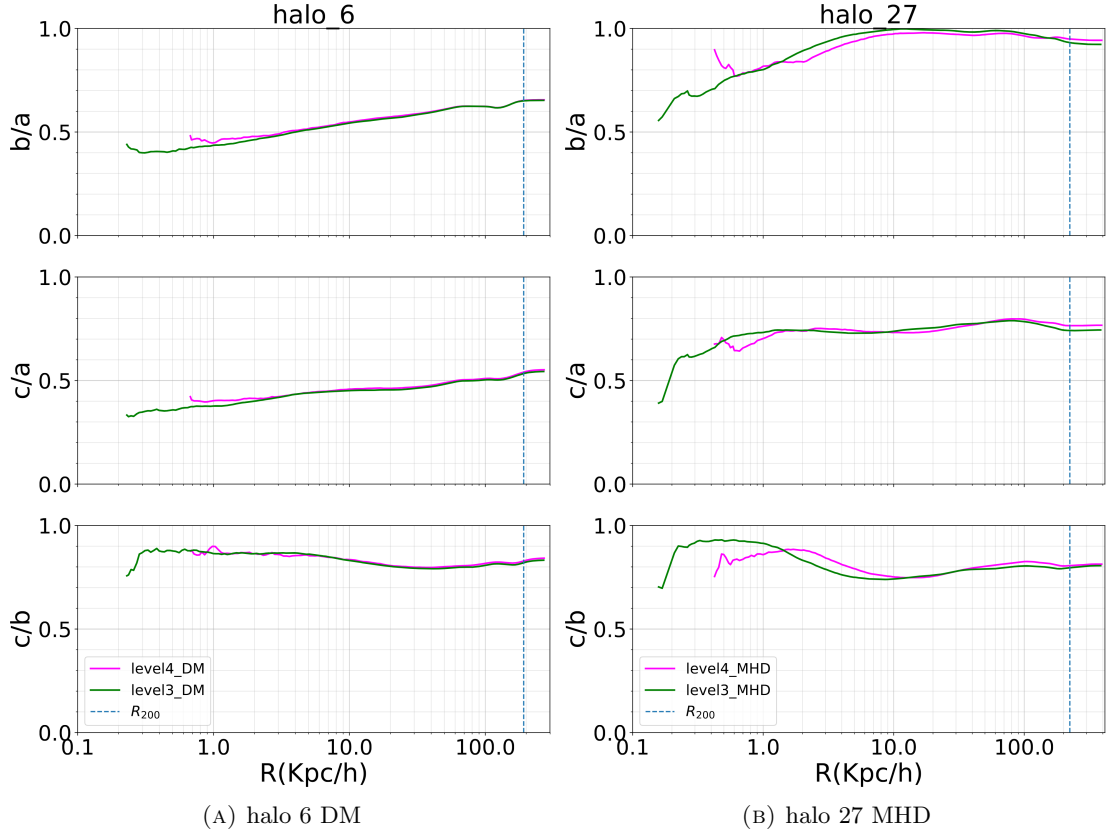


FIGURE 3.1: Level 3 (green) & 4 (pink) radial profiles of axial ratios for halo 6 (DM) & 21 (MHD). Here, it is clear that there is good agreement on the calculated quantities for both levels of resolution.

For instance, by simple inspection, we notice that there is no apparent systematic way in which resolution affects the halo shape. That is, sometimes the highly-resolved halo appears rounder and other times it seems more triaxial. This is important for our study as we focus on the analysis of the triaxial properties of the halo. Incidentally, DM-only halos remain unchanged with the exemption of the radial regimes where the number of particles affects our shape-calculating method. However, for MHD simulations, the resolution of gas has a global influence over the axial ratios. We suspect this is caused by continuous exposition of particles to the resolution-sensible baryonic potential. Nevertheless, further calculations are needed to confirm the cause of these discrepancies.

Consequently, to rule out our shape method as a cause of these resolution differences, we decide to isolate the few-particle effect on our calculations. To do this, we randomly select DM particles from level 3 halos at  $z = 0$  to produce 10 samples of approximately the same size as level 4 simulations. We then calculate this few-particle effect, which we show in figures 3.3. For each radius, we calculate the standard deviation of the sample

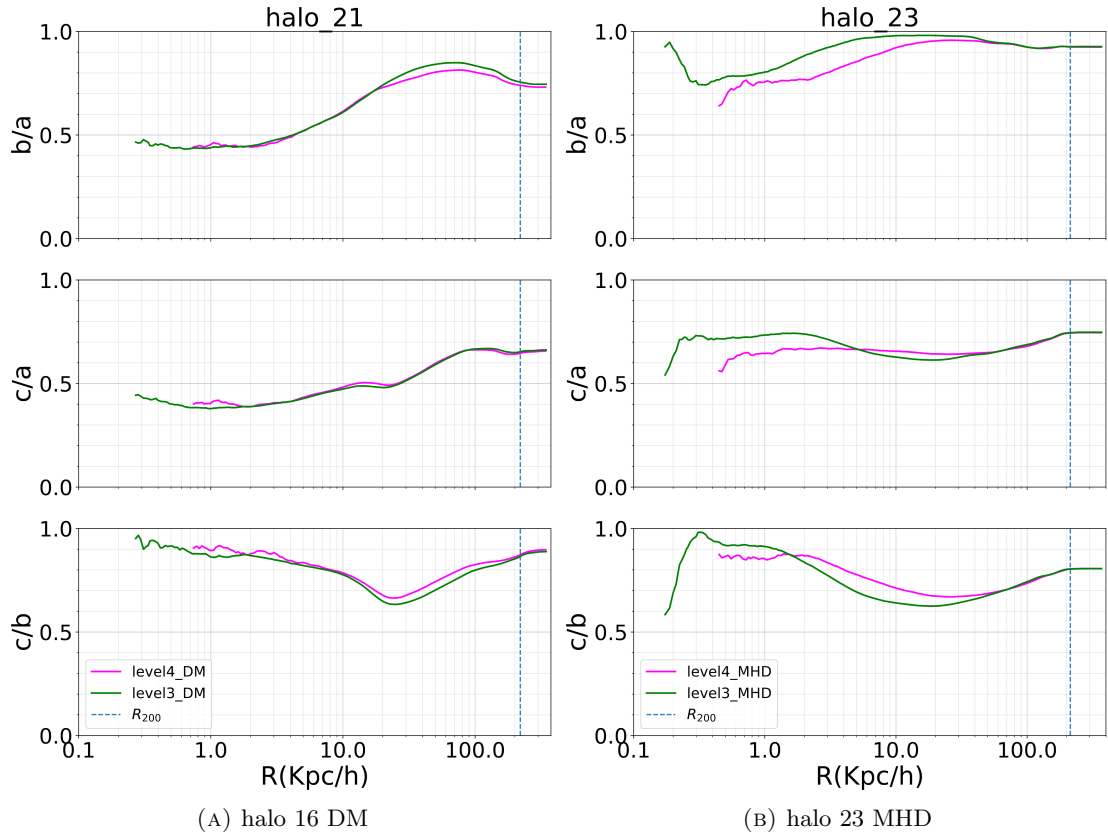


FIGURE 3.2: Level 3 (green) & 4 (pink) radial profiles of axial ratios for halo 16 (DM) & 23 (MHD). Here, axial ratios show slow convergence.

shape and illustrate a 3-sigma range around the level 3 curve to compare with the respective level 4 shape values.

From graphics on 3.3, it is clear that the fractional difference is not actually significant and remains under 1% for the majority of the radial profile. It becomes important for radii less than  $1Kpc$  due to the lack of particles for approximating an elliptical shape. This is corroborated by the  $3\sigma$  range, which also becomes evident around  $1Kpc$ . We deduce from this analysis that for radii bigger than  $1Kpc$ , the differences of level 3 and level 4 ellipses cannot be explained as an effect of the lack of particles. This is a confirmation that all kinds of matter are directly affected by resolution due to precision-sensitive events on the history of formation or because the numerical gravitational potential of matter continuously influences surrounding structures. Either way, even for the most resolution-biased cases, we can say that for the purposes of this study, convergence is achieved to a reasonable extent.

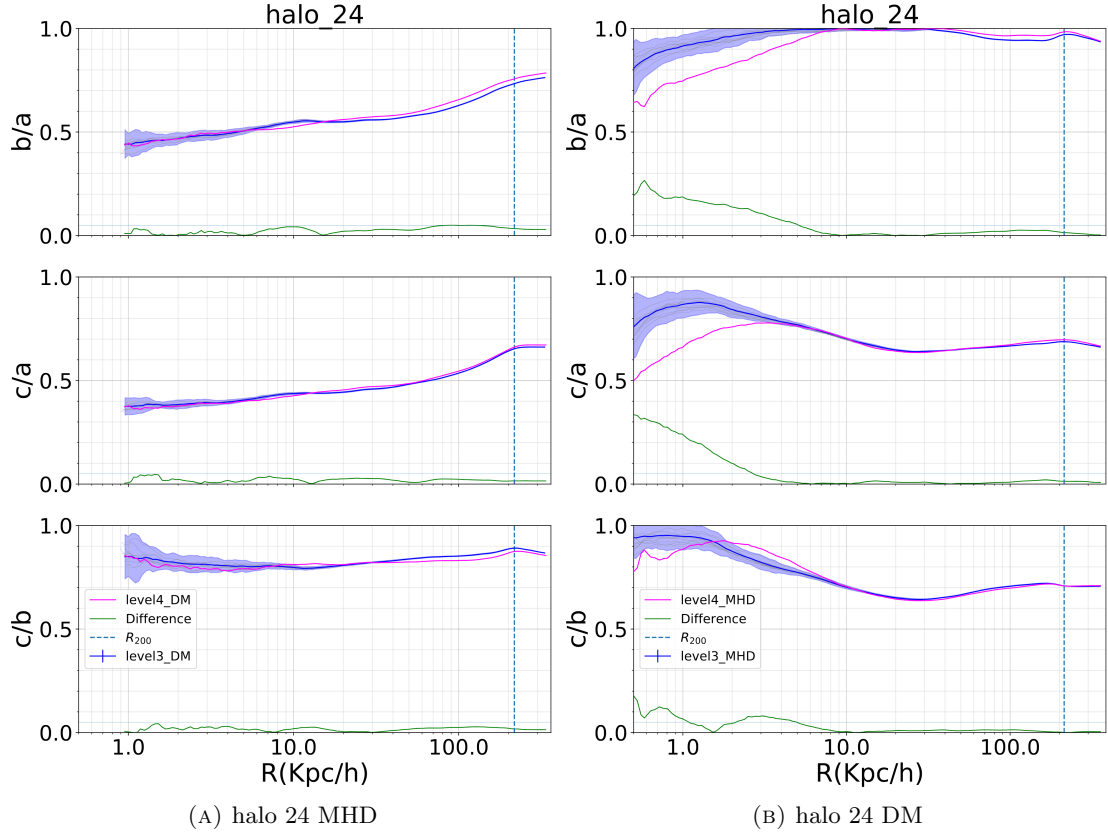


FIGURE 3.3: The few-particle effect on the axial ratios convergence for halo 24 (DM & MHD). Here level4 curves (magenta) are compared to the  $3\sigma$  range (clear blue) of the random-sampled curves from level3 (solid blue). We deduce from the fractional difference (green) that discrepancies at  $r >> 1\text{Kpc}$  cannot be explained solely with the few-particle bias.

### 3.2 The radial dependence of axial ratios

One of the our first results is related to the evolution of the DM halo shape in terms of the radius. We expect from previous work that the shape does not remain constant along the radius [38]. Specifically, after some time, halos are gradually constructed from inner shells to outer shells through constant accretion of matter from cosmic structures [59, 64]. Inner shells tend to conserve their shape as a consequence of being shielded from the outside by Gauss law. Outer shells, on the other side, are continuously affected by the gravitational potential from the inside, which makes them prone to shifting orbits. This inner gravitational potential has a *rounding* effect on the outskirts. For this reason, we expect that halos are more triaxial on inner regions and more spherical at bigger radii. This effect has been corroborated on multiple cosmological simulations [38, 65–70].

In figures 3.4, we present a halo in which this rounding effect is evident for both degrees of realism. However, to eliminate any possible qualitative bias, on figure 3.5 we present

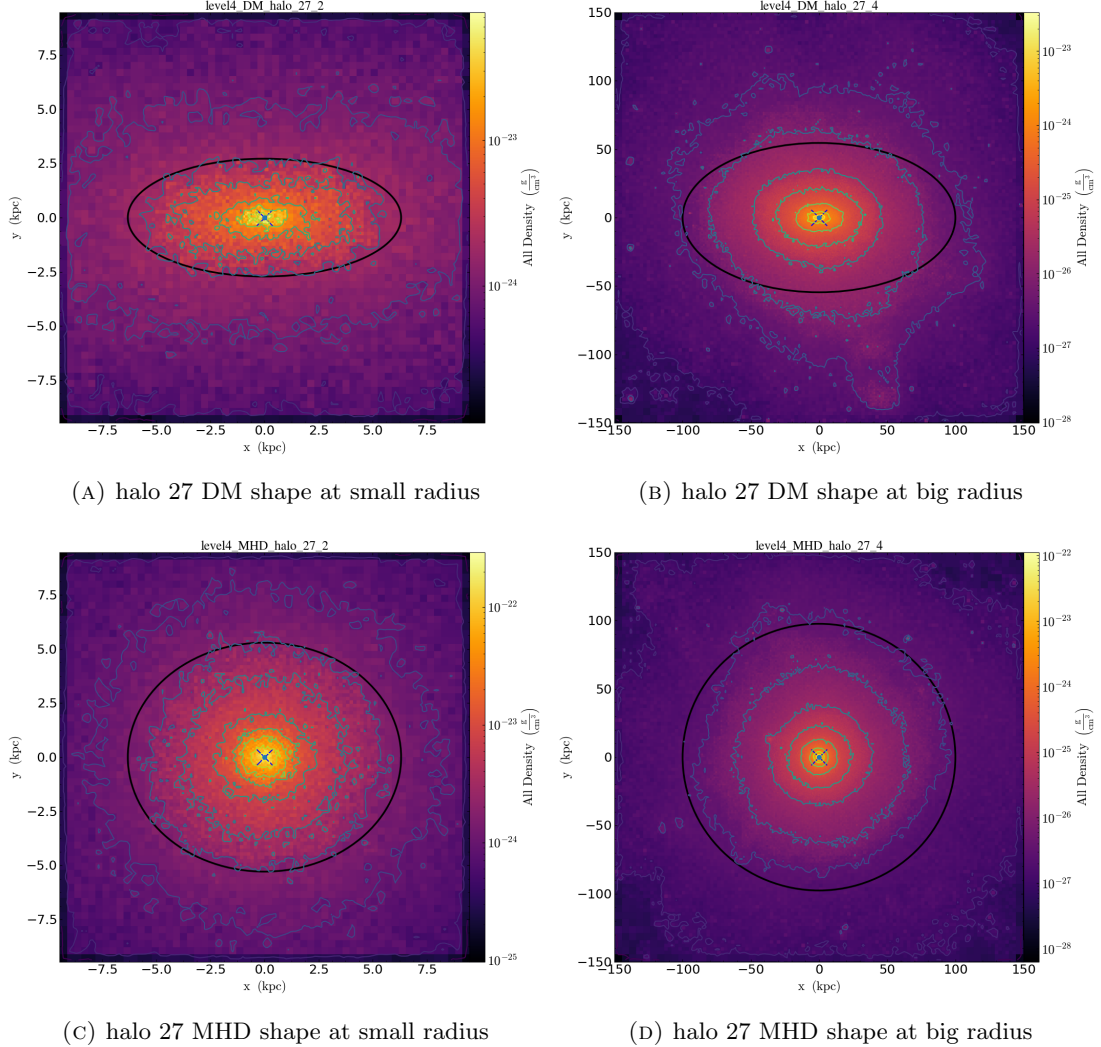


FIGURE 3.4: DM density for inner (left) and outer (right) parts of the halo 27. We present both versions: DM (up) & MHD (down). The horizontal and vertical axes are aligned to the major and medium semi-axes respectively. Here, it is evident that this halo is more spherical at bigger radii and more triaxial at the central parts.

a quantitative version of this effect. There, we include all axial ratios, which clearly become closer to 1 for bigger radii. Additionally, we include a quantification of the triaxiality, namely  $T = \frac{1-b/a}{1-c/a}$ .

This measurement  $T$  tends towards unity when the medium-to-major axis ratio becomes equal to the minor-to-major ratio, i.e. when the halo becomes prolate. When the medium axis is close to the major axis but not to the minor axis,  $T$  tends to a null value, i.e. when the halo tends to an oblate shape. In these terms, halos are expected to be more prolate on the inside and more oblate on the outside. Even though the perfect spherical shape has a divergent/undefined  $T$  value, prolate shapes are associated with triaxial characterizations and oblate shapes are identified as approximately spherical

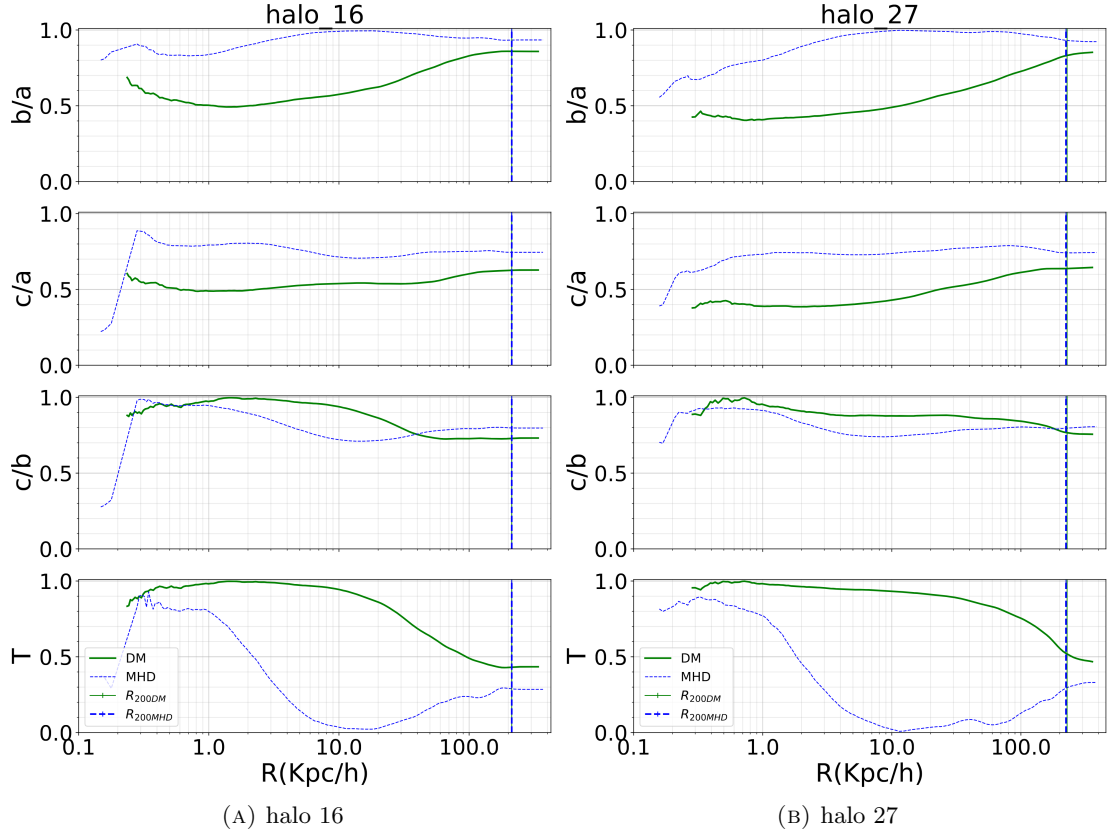


FIGURE 3.5: Radial profile for axial ratios and the triaxiality parameter  $T = \frac{1-b/a}{1-c/a}$  from halo 27 and halo 16. These halos have a clear radial tendency towards sphericity (for smaller radii until  $\approx 3\text{Kpc}$ ), which can be confirmed with the triaxiality parameter.

shapes. However, this can be confirmed on the triaxial  $c/a$  Vs  $b/a$  plane where we also demonstrate that this is in fact a global tendency for all halos.

In figure 3.6, we show the axial ratios on the plane  $c/a$  vs  $b/a$ . There, each dot labeled by radius represents a specific shape. In this plane, oblate halos are represented by the vertical line  $x = 1$ , prolate halos are identified on the identity line and spheres are exactly the point  $(1, 1)$ . This gives us a broader idea of the evolution of the shape. The tendency is clear for halos to get rounder with increasing radius. In fact, the difference in shape is clear enough that it is possible to identify groups in case the radius label is lost.

### 3.2.1 The effect of gas on the halo shape

We have simultaneously corroborated the rounding effect of radius on the halo shape from DM-only and MHD simulations. However, from the parallel presentation of results from MHD and DM simulations in previous figures, it is noticeable that MHD halos are

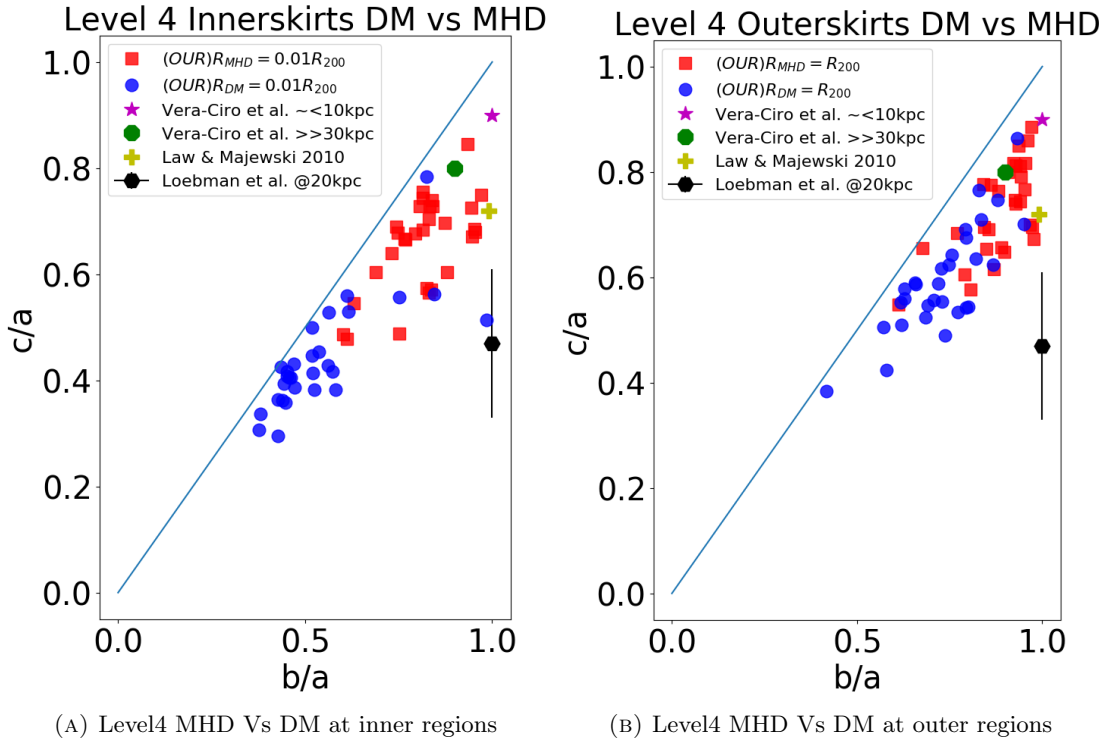


FIGURE 3.6: Axial ratios as shown on  $c/a$  Vs  $b/a$ . Each dot represents a halo shape at some radius. Some observational constraints are plotted alongside our results. Here, dots are clustered, proving the general tendency of halos to get rounder on the outer parts.

in general more spherical than DM halos, which is to be expected [71–73].

Unlike DM, gas collapses and generates disks which are much denser than the DM structures. This amplifies the effect of the gravitational potential and, if we apply the same logic, we would expect that the inner regions of the halo are more spherical where there is presence of gas. We expect the same for outer regions but this effect is predicted to be less significant due to the weaker effect of the gravitational potential of inner shells.

For instance, recurring again to the figures 3.4, now comparing the graphics vertically, the rounding effect of visible matter is clear. For a more quantitative illustration of this, we can refer to figure 3.5.

Although from previous pictures it is evident that the presence of gas affects the halo shape making it rounder, it is not clear that this effect is amplified for smaller radii. To confirm this, we recur again to triaxiality plane on 3.7, where this tendency becomes

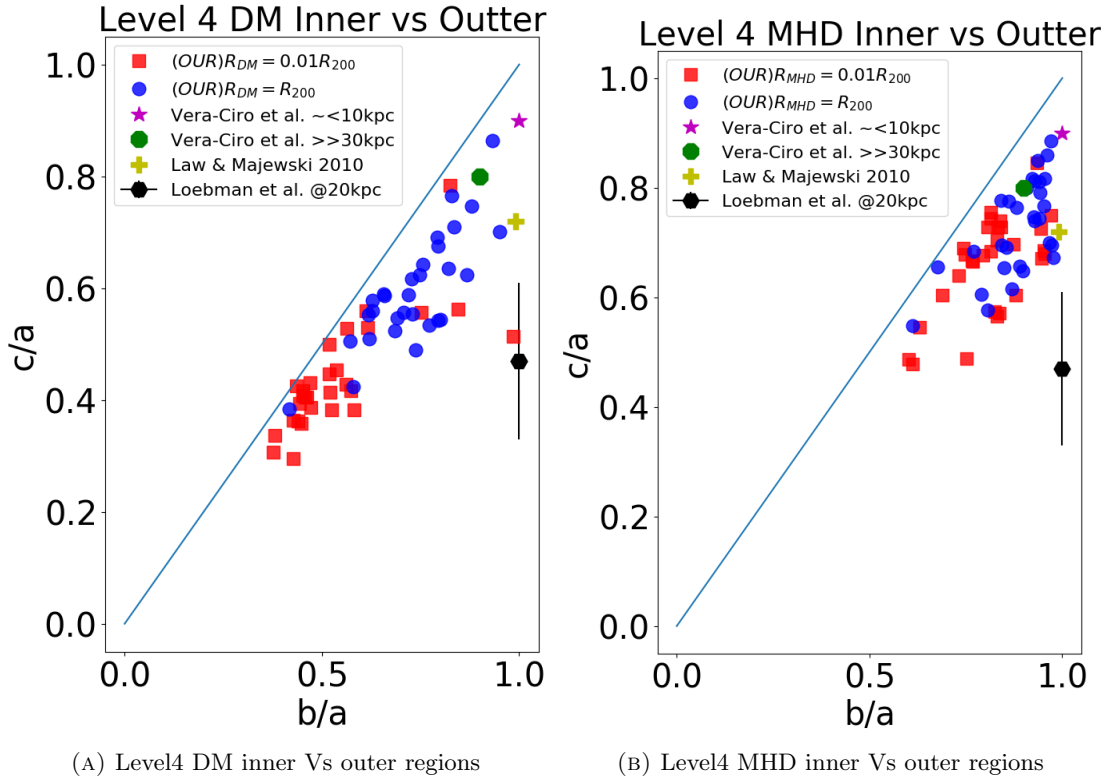


FIGURE 3.7: General tendency on the triaxial plane  $c/a$  Vs  $b/a$ . Some observational constraints are plotted alongside our results

evident.

So far, our results are in accordance with previous work. Nonetheless, in the specific case of MW-like galaxy simulations, we have confirmed the expected tendency in an unprecedented statistically significant sample of 30 galaxies from Auriga, compared to the 4-sample galaxies from the previous state-of-the-art Aquarius simulations. Moreover, we confirmed that these results are sustained for the specific case of novel MHD MW-like galaxy simulations where we could also analyze the effect of gas.

### 3.3 Historical shape

Taking into account the previous phenomenology for halo formation, it is possible to extend its reach for the analysis of the historical evolution of the halo shape.

Recalling that inner shells of the halo are isolated from the gravitational effect of outer shells, the only significant source of disruption in time of this radial regime are external

structures that perform some torque on them. Outer shells must feel this source of deformation too in addition to the effect from the inner gravitational potential. Consequently, we expect a systematic change on the halo shape with time, which becomes more significant for bigger radii.

Major events like mergers, may completely disturb a galaxy shapes and erase any memory of it. However, from  $z \approx 1$  onwards, these events are very rare [64] and we expect that any source of disruption is weak and is reduced to the previously mentioned factors. These sources of potential asymmetries influence DM particles towards more spherical orbits [44].

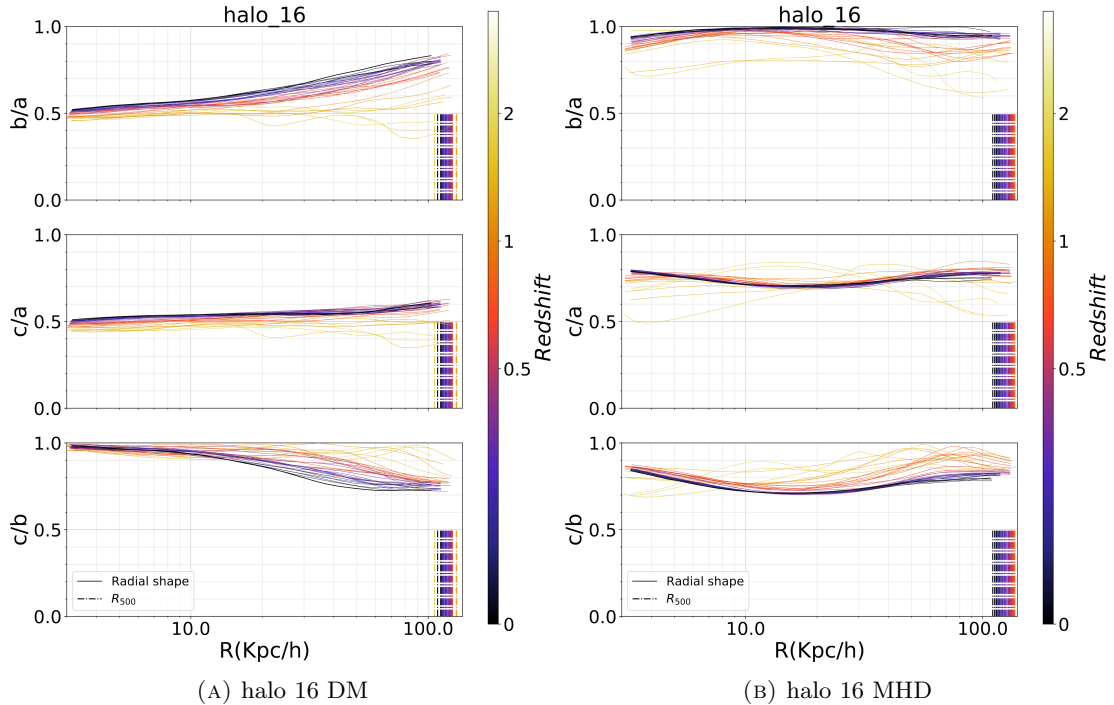


FIGURE 3.8: Radial profile (comoving) of axial ratios for halo 16 in terms of redshift (color). This halo maintains its shape until  $z \approx 1$  obviating the systematic rounding effect in time from asymmetric potentials.

In figures 3.8 we present the evolution of the radial profile of the shape of a halo that managed to conserve its integrity until  $z \approx 1$ . In this case, we show our results in terms of the comoving coordinates to obviate the scale factor and make these profiles comparable. The halo becomes systematically more spherical as it evolves in time, being this effect more relevant for  $r > 50Kpc$ .

In figures we present a special case of a halo that was perturbed at some time around  $z \approx 0.5$ . It is specially evident because of the discontinuity caused in the radial profile and the large differences in the virial radii.

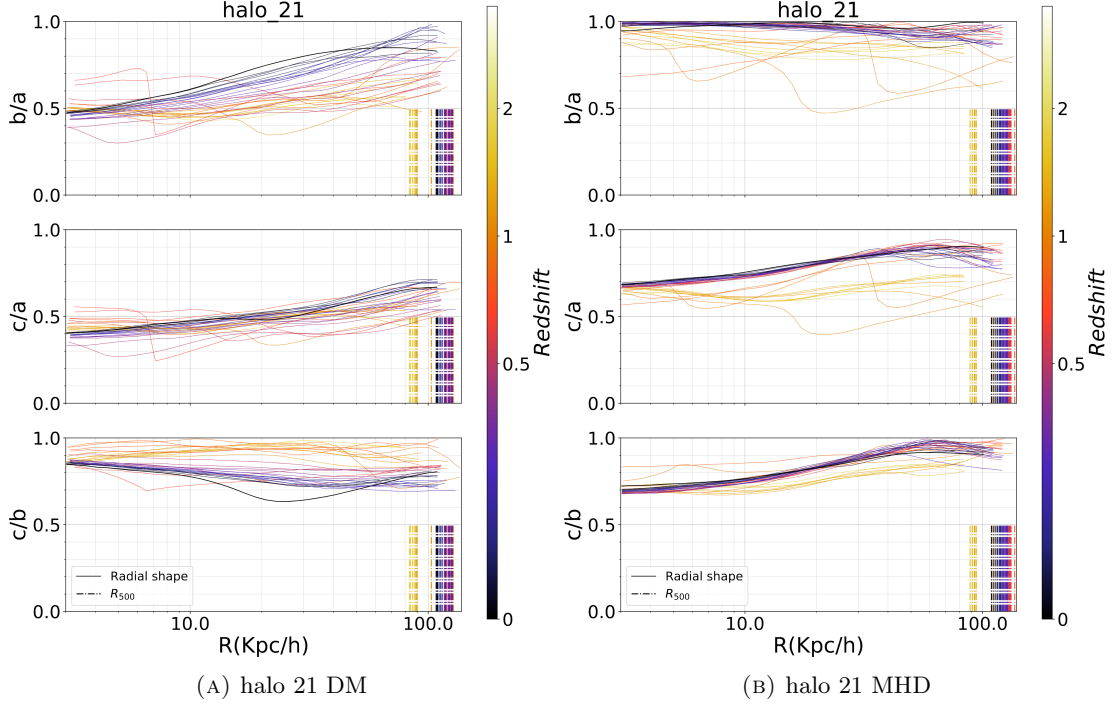


FIGURE 3.9: Radial profile (comoving) of axial ratios for halo 21 in terms of redshift (color). This halo is disrupted around  $z \approx 0.5$  which results in a certain loss of its shape memory.

Now, these results compare radial profiles in comoving coordinates, but in real life we have physical coordinates. In this order of ideas, we can state this preservation of the shape (obviating the rounding effect) without recurring to comoving comparisons.

In this case, consider a physical radius  $R$  that is well-defined for each redshift, at which we are going to perform our historical measurements. For practical purposes let us take, for example, the virial radius at each redshift. From  $z \approx 1$  onwards, mass accretion is in general steady and slow, and therefore, the virial radius will not experience significant variations in comoving coordinates. Given that there is a systematic tendency for the halo to get more spherical with time, and that this tendency is stronger for outskirts, e.g. the virial radius, this means that by sampling the axial ratios at the virial radius at each redshift, we are effectively sampling the shape for smaller radii at  $z = 0$ . Therefore, we expect that the historical profile of the axial ratios at the physical virial radius is correlated to the radial profile at the present time.

To illustrate this, in figures 3.10 we present the historical and radial profiles of the previously analyzed halo shapes. For the halo that maintained a consistent shape during time, there is a clear correlation between the historical and radial profiles, both clearly tending to more spherical shapes at lower redshifts and bigger radii. In the case of the halo that had a major disrupting event, this correlation is not clear as an evidence of memory loss by the massive infalling material.

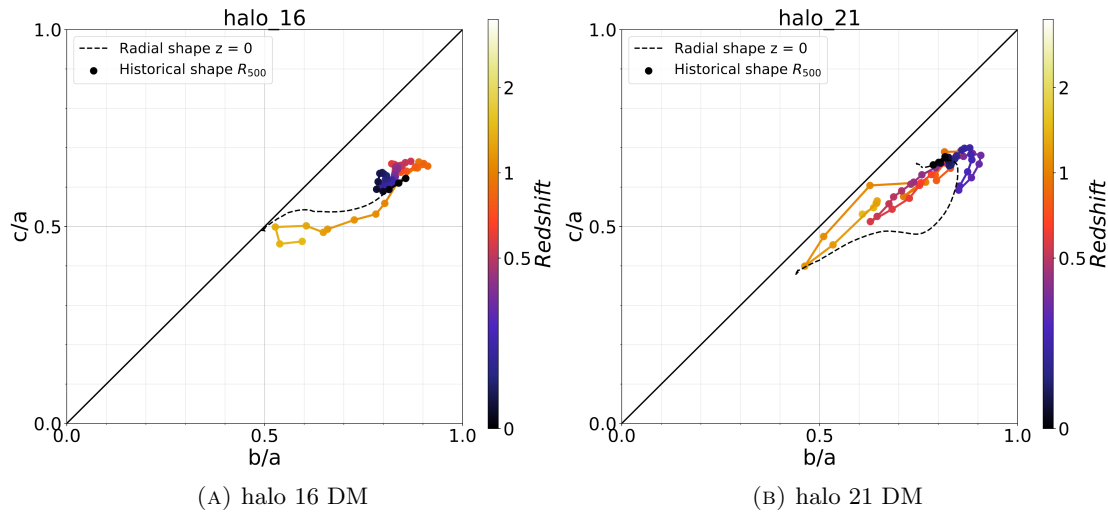


FIGURE 3.10: Historic shape (color dots) Vs actual radial shape (solid black line) on the Triaxiality plane. Each colored dot represents a calculated shape at R Mean 200, for each redshift. It is clear that halos with memory (halo 16), unlike disrupted halos (halo 21), have correlation between their historical and radial profiles.

## Chapter 4

# Conclusions

Our work on the expected shape of DM halos is motivated by various factors. On one hand, obtained insight on the halo shape of full-physics MW-like simulations like Auriga [55] may be applied to the improvement of constraints on the DM density field of our MW. This would result in a better comprehension of the behaviour and nature of DM itself. On the other hand, the novelty of gas models in Auriga simulations, which we exploit, makes them unique for the understanding of the effect visible matter on the axial ratios of DM halos. Given the vast work on DM-only simulations, our results could be applied to make more realistic conclusions on these previous studies. Finally, the unique significant sample of 30 high-resolution galaxies from the Auriga project makes our results statistically-supported and may be used to obtain better understanding of random biases that may affect works of this kind.

In this work we use Allgood’s method for shape calculation [63] on the 30-sized set of DM-only and MHD MW-like simulations from the Auriga [55] project to verify the results obtained by [38, Vera-Ciro et al. 2011] about the shape of DM halos from Aquarius simulations and obtain more insight about how DM halos behave on MW-like galaxy simulations. Auriga includes consistent models for energetic and accretion feedback from stars and Black Holes and the unique inclusion of magnetic fields. These models worked over a significant set of 30 galaxies evolved with the Arepo code [56], which solves the principal problems of the previous Computational Fluid Dynamics paradigms. All these properties make of Auriga one of the most advanced and precise set of simulations in actuality.

Taking this into account, we verify that, at  $z = 0$ , DM halos from DM-only and MHD simulations are more oblate/spherical on outer regions and more prolate/triaxial on inner parts. We corroborate this effect in different manners, by obtaining the radial profile of the axial ratios, calculating a triaxiality indicator  $T$  and presenting our results on the triaxial plane. Although our results were expected from the work on various cosmological simulations [38, 65–70], our study is supported with an unprecedented sample of 30 level 4 resolution MW-like simulated galaxies.

Taking advantage of the parallel outcome of DM-only and MHD versions of the same galaxies on Auriga, we compare both versions to analyze the effect of the presence of gas on the shape of the DM halos. We find that gas affects the shape at all radii by making the halo more spherical. Furthermore, we demonstrate that this rounding effect is more prominent on the inner regions of the halo. These results are also in agreement with previous studies on this subject [71–73].

Vera-Ciro et al. deduced by inspection and showed that there is a correlation between the radial profile of the halo's axial ratios and the historical evolution at a determined radius. We corroborate this fact for DM-only simulations and show the reason for this correlation by calculating the radial shapes at comoving coordinates. We discover that the shape remains more or less unchanged in time once we account for the continuous rounding effect which is shown to be more prominent on the outskirts of the halo, due to the continuous exposure to the inner gravitational potential. This systematic tendency towards sphericity is, together with the pronounced rounding effect at the outskirts of the halo is traduced in a correlation of the historical shape at the virial radius with the radial profile at  $z = 0$ .

We conclude our study by stating some interesting questions and proposing further studies on this matter. First, this work may be extended to the analysis of the impact of environmental structures on the shape of the DM halo where it is of special interest the study of the relation of shapes with angular momentum and the orientation of the principal axes of the halo with respect to those determined by cosmic structures. Furthermore, we could make use of the exceptional number of simulated galaxies to address statistical problems such as the verification and improvement of theoretical models that predict the response of DM halos to the presence of matter, like adiabatic contractions [74].

# Bibliography

- [1] F. Zwicky. On the Masses of Nebulae and of Clusters of Nebulae. *The Astrophysics Journal*, 86:217, October 1937. doi: 10.1086/143864.
- [2] S. M. Faber and J. S. Gallagher. Masses and mass-to-light ratios of galaxies. *Annual Review of Astronomy and Astrophysics*, 17:135–187, 1979. doi: 10.1146/annurev.aa.17.090179.001031.
- [3] V. C. Rubin, W. K. Ford, Jr., and N. Thonnard. Rotational properties of 21 SC galaxies with a large range of luminosities and radii, from NGC 4605 /R = 4kpc/ to UGC 2885 /R = 122 kpc/. *The Astrophysics Journal*, 238:471–487, June 1980. doi: 10.1086/158003.
- [4] M. Persic, P. Salucci, and F. Stel. The universal rotation curve of spiral galaxies - I. The dark matter connection. *Monthly Notices of the Royal Astronomical Society*, 281:27–47, July 1996. doi: 10.1093/mnras/281.1.27.
- [5] N. Kaiser and G. Squires. Mapping the dark matter with weak gravitational lensing. *The Astrophysics Journal*, 404:441–450, February 1993. doi: 10.1086/172297.
- [6] D. M. Wittman, J. A. Tyson, D. Kirkman, I. Dell’Antonio, and G. Bernstein. Detection of weak gravitational lensing distortions of distant galaxies by cosmic dark matter at large scales. *Nature*, 405:143–148, May 2000. doi: 10.1038/35012001.
- [7] D. Clowe, M. Bradav c, A. H. Gonzalez, M. Markevitch, S. W. Randall, C. Jones, and D. Zaritsky. A Direct Empirical Proof of the Existence of Dark Matter. *The Astrophysics Journall*, 648:L109–L113, September 2006. doi: 10.1086/508162.
- [8] George R Blumenthal, SM Faber, Joel R Primack, and Martin J Rees. Formation of galaxies and large-scale structure with cold dark matter. *Nature*, 311(5986):517, 1984.
- [9] David N Spergel, Licia Verde, Hiranya V Peiris, E Komatsu, MR Nolta, CL Bennett, M Halpern, G Hinshaw, N Jarosik, A Kogut, et al. First-year wilkinson microwave anisotropy probe (wmap)\* observations: determination of cosmological parameters. *The Astrophysical Journal Supplement Series*, 148(1):175, 2003.

- [10] Gary Hinshaw, D Larson, Eiichiro Komatsu, DN Spergel, CLaa Bennett, J Dunkley, MR Nolta, M Halpern, RS Hill, N Odegard, et al. Nine-year wilkinson microwave anisotropy probe (wmap) observations: cosmological parameter results. *The Astrophysical Journal Supplement Series*, 208(2):19, 2013.
- [11] Peter AR Ade, N Aghanim, C Armitage-Caplan, M Arnaud, M Ashdown, F Atrio-Barandela, J Aumont, C Baccigalupi, Anthony J Banday, RB Barreiro, et al. Planck 2013 results. xvi. cosmological parameters. *Astronomy and Astrophysics*, 571:A16, 2014.
- [12] Peter AR Ade, N Aghanim, M Arnaud, M Ashdown, J Aumont, C Baccigalupi, AJ Banday, RB Barreiro, JG Bartlett, N Bartolo, et al. Planck 2015 results-xiii. cosmological parameters. *Astronomy and Astrophysics*, 594:A13, 2016.
- [13] Mordehai Milgrom. A modification of the newtonian dynamics as a possible alternative to the hidden mass hypothesis. *The Astrophysical Journal*, 270:365–370, 1983.
- [14] Robert H Sanders and Stacy S McGaugh. Modified newtonian dynamics as an alternative to dark matter. *Annual Review of Astronomy and Astrophysics*, 40(1):263–317, 2002.
- [15] KG Begeman, AH Broeils, and RH Sanders. Extended rotation curves of spiral galaxies: Dark haloes and modified dynamics. *Monthly Notices of the Royal Astronomical Society*, 249(3):523–537, 1991.
- [16] S. S. McGaugh and W. J. G. de Blok. Testing the Hypothesis of Modified Dynamics with Low Surface Brightness Galaxies and Other Evidence. *The Astrophysics Journal*, 499:66–81, May 1998. doi: 10.1086/305629.
- [17] Stacy S. McGaugh. The Baryonic Tully-Fisher Relation of Gas-rich Galaxies as a Test of  $\Lambda$ CDM and MOND. *The Astronomical Journal*, 143:40, February 2012. doi: 10.1088/0004-6256/143/2/40.
- [18] Ewa L Lokas. Dark matter distribution in dwarf spheroidal galaxies. *Monthly Notices of the Royal Astronomical Society*, 333(3):697–708, 2002.
- [19] S. S. McGaugh. A tale of two paradigms: the mutual incommensurability of  $\Lambda$ CDM and MOND. *Canadian Journal of Physics*, 93:250–259, February 2015. doi: 10.1139/cjp-2014-0203.
- [20] Jihn E Kim. Light pseudoscalars, particle physics and cosmology. *Physics Reports*, 150(1-2):1–177, 1987.

- [21] Gianfranco Bertone, Dan Hooper, and Joseph Silk. Particle dark matter: Evidence, candidates and constraints. *Physics Reports*, 405(5-6):279–390, 2005.
- [22] J Richard Bond, George Efstathiou, and Joseph Silk. Massive neutrinos and the large-scale structure of the universe. *Physical Review Letters*, 45(24), 1980.
- [23] Andrew R Liddle and David H Lyth. The cold dark matter density perturbation. *Physics Reports*, 231(1-2):1–105, 1993.
- [24] Paul Schechter. An analytic expression for the luminosity function for galaxies. *The Astrophysical Journal*, 203:297–306, 1976.
- [25] J. M. Bardeen, J. R. Bond, N. Kaiser, and A. S. Szalay. The statistics of peaks of Gaussian random fields. *The Astrophysics Journal*, 304:15–61, May 1986. doi: 10.1086/164143.
- [26] J. F. Navarro, C. S. Frenk, and S. D. M. White. The Structure of Cold Dark Matter Halos. *The Astrophysics Journal*, 462:563, May 1996. doi: 10.1086/177173.
- [27] J. F. Navarro, C. S. Frenk, and S. D. M. White. A Universal Density Profile from Hierarchical Clustering. *The Astrophysics Journal*, 490:493–508, December 1997. doi: 10.1086/304888.
- [28] Chris Power, JF Navarro, A Jenkins, CS Frenk, Simon DM White, V Springel, J Stadel, and T Quinn. The inner structure of  $\lambda$  cdm haloes-i. a numerical convergence study. *Monthly Notices of the Royal Astronomical Society*, 338(1):14–34, 2003.
- [29] Julio F Navarro, Aaron Ludlow, Volker Springel, Jie Wang, Mark Vogelsberger, Simon DM White, Adrian Jenkins, Carlos S Frenk, and Amina Helmi. The diversity and similarity of simulated cold dark matter haloes. *Monthly Notices of the Royal Astronomical Society*, 402(1):21–34, 2010.
- [30] James E Gunn and J Richard Gott III. On the infall of matter into clusters of galaxies and some effects on their evolution. *The Astrophysical Journal*, 176:1, 1972.
- [31] S. D. M. White and D. Zaritsky. Models for Galaxy halos in an open universe. *The Astrophysics Journal*, 394:1–6, July 1992. doi: 10.1086/171552.
- [32] J. H. Jeans. On the theory of star-streaming and the structure of the universe. *Monthly Notices of the Royal Astronomical Society*, 76:70–84, December 1915. doi: 10.1093/mnras/76.2.70.

- [33] S.R. Loebman, v Z. Ivezić, T.R. Quinn, F. Governato, A.M. Brooks, C.R. Christensen, and M. Juric. Constraints on the Shape of the Milky Way Dark Matter Halo from Jeans Equations Applied to Sloan Digital Sky Survey Data. *The Astrophysics Journal, Letters*, 758:L23, October 2012. doi: 10.1088/2041-8205/758/1/L23.
- [34] J. I. Read and Ben Moore. Tidal streams in a monod potential: constraints from sagittarius. *Monthly Notices of the Royal Astronomical Society*, 361(3):971–976, 2005. doi: 10.1111/j.1365-2966.2005.09232.x. URL [+http://dx.doi.org/10.1111/j.1365-2966.2005.09232.x](http://dx.doi.org/10.1111/j.1365-2966.2005.09232.x).
- [35] C. Nipoti, P. Londrillo, H. Zhao, and L. Ciotti. Vertical dynamics of disc galaxies in modified Newtonian dynamics. *Monthly Notices of the Royal Astronomical Society*, 379:597–604, August 2007. doi: 10.1111/j.1365-2966.2007.11835.x.
- [36] J. I. Read, G. Lake, O. Agertz, and Victor P. Debattista. Thin, thick and dark discs in cdm. *Monthly Notices of the Royal Astronomical Society*, 389(3):1041–1057, 2008. doi: 10.1111/j.1365-2966.2008.13643.x. URL [+http://dx.doi.org/10.1111/j.1365-2966.2008.13643.x](http://dx.doi.org/10.1111/j.1365-2966.2008.13643.x).
- [37] J.I. Read, L. Mayer, A.M. Brooks, F. Governato, and G. Lake. A dark matter disc in three cosmological simulations of Milky Way mass galaxies. *Monthly Notices of the Royal Astronomical Society*, 397:44–51, July 2009. doi: 10.1111/j.1365-2966.2009.14757.x.
- [38] C.A. Vera-Ciro, L.V. Sales, A. Helmi, C.S. Frenk, J.F. Navarro, V. Springel, M. Vo-gelsberger, and S.D.M. White. The shape of dark matter haloes in the Aquarius simulations: evolution and memory. *Monthly Notices of the Royal Astronomical Society*, 416:1377–1391, September 2011. doi: 10.1111/j.1365-2966.2011.19134.x.
- [39] C. Vera-Ciro and A. Helmi. Constraints on the Shape of the Milky Way Dark Matter Halo from the Sagittarius Stream. *The Astrophysics Journal, Letters*, 773:L4, August 2013. doi: 10.1088/2041-8205/773/1/L4.
- [40] David R Law, Steven R Majewski, and Kathryn V Johnston. Evidence for a tri-axial milky way dark matter halo from the sagittarius stellar tidal stream. *The Astrophysical Journal Letters*, 703(1):L67, 2009.
- [41] D. R. Law and S. R. Majewski. The Sagittarius Dwarf Galaxy: A Model for Evolution in a Triaxial Milky Way Halo. *The Astrophysics Journal*, 714:229–254, May 2010. doi: 10.1088/0004-637X/714/1/229.
- [42] Nathan Deg and Lawrence Widrow. The Sagittarius stream and halo triaxiality. *Monthly Notices of the Royal Astronomical Society*, 428:912–922, January 2013. doi: 10.1093/mnras/sts089.

- [43] Masanori Miyamoto and Ryuzaburo Nagai. Three-dimensional models for the distribution of mass in galaxies. *Publications of the Astronomical Society of Japan*, 27:533–543, 1975.
- [44] Victor P Debattista, Ben Moore, Thomas Quinn, Stelios Kazantzidis, Ryan Maas, Lucio Mayer, Justin Read, and Joachim Stadel. The causes of halo shape changes induced by cooling baryons: disks versus substructures. *The Astrophysical Journal*, 681(2):1076, 2008.
- [45] Jeremiah Paul Ostriker and Philip JE Peebles. A numerical study of the stability of flattened galaxies: or, can cold galaxies survive? *The Astrophysical Journal*, 186:467–480, 1973.
- [46] R. H. Miller and K. H. Prendergast. Stellar Dynamics in a Discrete Phase Space. *The Astrophysics Journal*, 151:699, February 1968. doi: 10.1086/149469.
- [47] Frank Hohl and RW Hockney. A computer model of disks of stars. *Journal of Computational Physics*, 4(3):306–324, 1969.
- [48] R. H. Miller, K. H. Prendergast, and W. J. Quirk. Numerical Experiments on Spiral Structure. *The Astrophysics Journal*, 161:903, September 1970. doi: 10.1086/150593.
- [49] A. Toomre and J. Toomre. Galactic Bridges and Tails. *The Astrophysics Journal*, 178:623–666, December 1972. doi: 10.1086/151823.
- [50] Josh Barnes and Piet Hut. A hierarchical  $O(n \log n)$  force-calculation algorithm. *nature*, 324(6096):446, 1986.
- [51] Marsha J Berger and Phillip Colella. Local adaptive mesh refinement for shock hydrodynamics. *Journal of computational Physics*, 82(1):64–84, 1989.
- [52] G. Lemson and t. Virgo Consortium. Halo and Galaxy Formation Histories from the Millennium Simulation: Public release of a VO-oriented and SQL-queryable database for studying the evolution of galaxies in the LambdaCDM cosmogony. *ArXiv Astrophysics e-prints*, August 2006.
- [53] G. De Lucia, V. Springel, S. D. M. White, D. Croton, and G. Kauffmann. The formation history of elliptical galaxies. *Monthly Notices of the Royal Astronomical Society*, 366:499–509, February 2006. doi: 10.1111/j.1365-2966.2005.09879.x.
- [54] Neal Katz and James E Gunn. Dissipational galaxy formation. i-effects of gasdynamics. *The Astrophysical Journal*, 377:365–381, 1991.

- [55] R. J. J. Grand, F. A. Gomez, F. Marinacci, R. Pakmor, V. Springel, D. J. R. Campbell, C. S. Frenk, A. Jenkins, and S. D. M. White. The Auriga Project: the properties and formation mechanisms of disc galaxies across cosmic time. *Monthly Notices of the Royal Astronomical Society*, 467:179–207, May 2017. doi: 10.1093/mnras/stx071.
- [56] V. Springel. E pur si muove: Galilean-invariant cosmological hydrodynamical simulations on a moving mesh. *Monthly Notices of the Royal Astronomical Society*, 401:791–851, January 2010. doi: 10.1111/j.1365-2966.2009.15715.x.
- [57] R. Pakmor, F. A. Gomez, R. J. J. Grand, F. Marinacci, C. M. Simpson, V. Springel, D. J. R. Campbell, C. S. Frenk, T. Guillet, C. Pfrommer, and S. D. M. White. Magnetic field formation in the Milky Way-like disk galaxies of the Auriga project. *ArXiv e-prints*, January 2017.
- [58] V. Springel, J. Wang, M. Vogelsberger, A. Ludlow, A. Jenkins, A. Helmi, J. F. Navarro, C. S. Frenk, and S. D. M. White. The Aquarius Project: the subhaloes of galactic haloes. *Monthly Notices of the Royal Astronomical Society*, 391:1685–1711, December 2008. doi: 10.1111/j.1365-2966.2008.14066.x.
- [59] Giuseppe Tormen, Francois R Bouchet, and Simon DM White. The structure and dynamical evolution of dark matter haloes. *Monthly Notices of the Royal Astronomical Society*, 286(4):865–884, 1997.
- [60] J. M. Colberg, S. D. M. White, A. Jenkins, and F. R. Pearce. Linking cluster formation to large-scale structure. *Monthly Notices of the Royal Astronomical Society*, 308:593–598, September 1999. doi: 10.1046/j.1365-8711.1999.02400.x.
- [61] J. Schaye, R. A. Crain, R. G. Bower, M. Furlong, M. Schaller, T. Theuns, C. Dalla Vecchia, C. S. Frenk, I. G. McCarthy, J. C. Helly, A. Jenkins, Y. M. Rosas-Guevara, S. D. M. White, M. Baes, C. M. Booth, P. Camps, J. F. Navarro, Y. Qu, A. Rahmati, T. Sawala, P. A. Thomas, and J. Trayford. The EAGLE project: simulating the evolution and assembly of galaxies and their environments. *Monthly Notices of the Royal Astronomical Society*, 446:521–554, January 2015. doi: 10.1093/mnras/stu2058.
- [62] M. Davis, G. Efstathiou, C. S. Frenk, and S. D. M. White. The evolution of large-scale structure in a universe dominated by cold dark matter. *The Astrophysics Journal*, 292:371–394, May 1985. doi: 10.1086/163168.
- [63] B. Allgood, R. A. Flores, J. R. Primack, A. V. Kravtsov, R. H. Wechsler, A. Faltenbacher, and J. S. Bullock. The shape of dark matter haloes: dependence on

- mass, redshift, radius and formation. *Monthly Notices of the Royal Astronomical Society*, 367:1781–1796, April 2006. doi: 10.1111/j.1365-2966.2006.10094.x.
- [64] Giuseppe Tormen, Antonaldo Diaferio, and David Syer. Survival of substructure within dark matter haloes. *Monthly Notices of the Royal Astronomical Society*, 299 (3):728–742, 1998.
- [65] Carlos S Frenk, Simon DM White, Marc Davis, and George Efstathiou. The formation of dark halos in a universe dominated by cold dark matter. *The Astrophysical Journal*, 327:507–525, 1988.
- [66] J. Dubinski and R. G. Carlberg. The structure of cold dark matter halos. *The Astrophysics Journal*, 378:496–503, September 1991. doi: 10.1086/170451.
- [67] Michael S Warren, Peter J Quinn, John K Salmon, and Wojciech H Zurek. Dark halos formed via dissipationless collapse. i-shapes and alignment of angular momentum. *The Astrophysical Journal*, 399:405–425, 1992.
- [68] S. Cole and C. Lacey. The structure of dark matter haloes in hierarchical clustering models. *Monthly Notices of the Royal Astronomical Society*, 281:716, July 1996. doi: 10.1093/mnras/281.2.716.
- [69] Eric Hayashi, Julio F Navarro, and Volker Springel. The shape of the gravitational potential in cold dark matter haloes. *Monthly Notices of the Royal Astronomical Society*, 377(1):50–62, 2007.
- [70] P. Bett, V. Eke, C. S. Frenk, A. Jenkins, J. Helly, and J. Navarro. The spin and shape of dark matter haloes in the Millennium simulation of a  $\Lambda$  cold dark matter universe. *Monthly Notices of the Royal Astronomical Society*, 376:215–232, March 2007. doi: 10.1111/j.1365-2966.2007.11432.x.
- [71] Joshua E Barnes and Lars Hernquist. Transformations of galaxies. ii. gasdynamics in merging disk galaxies. *The Astrophysical Journal*, 471(1):115, 1996.
- [72] V. Springel, S. D. M. White, and L. Hernquist. The shapes of simulated dark matter halos. In S. Ryder, D. Pisano, M. Walker, and K. Freeman, editors, *Dark Matter in Galaxies*, volume 220 of *IAU Symposium*, page 421, July 2004.
- [73] SE Bryan, ST Kay, AR Duffy, J Schaye, C Dalla Vecchia, and CM Booth. The impact of baryons on the spins and shapes of dark matter haloes. *Monthly Notices of the Royal Astronomical Society*, 429(4):3316–3329, 2013.
- [74] Oleg Y Gnedin, Andrey V Kravtsov, Anatoly A Klypin, and Daisuke Nagai. Response of dark matter halos to condensation of baryons: cosmological simulations

and improved adiabatic contraction model. *The Astrophysical Journal*, 616(1):16, 2004.